The *N*6-Methyl Group of Adenine Further Increases the BI Stability of DNA Compared to *C*5-Methyl Groups

Fajar R. Wibowo,[†] Michael Trieb, Christine Rauch, Bernd Wellenzohn, and Klaus R. Liedl*

Institute of General, Inorganic and Theoretical Chemistry, University of Innsbruck, Innrain 52a, A-6020 Innsbruck, Austria

Received: April 5, 2004; In Final Form: October 12, 2004

Methylated DNA bases are natural modifications which play an important role in protein−DNA interactions. Recent experimental and theoretical results have shown an influence of the base modification on the conformational behavior of the DNA backbone. MD simulations of four different B-DNA dodecamers ($d(GC)_6$, $d(AT)_6$, $d(G(5mCG)_5C)$, and $d(A(T6mA)_5T)$) have been performed with the aim to examine the influence of methyl groups on the B-DNA backbone behavior. An additional control simulation of $d(AU)_6$ has also been performed to examine the further influence of the *C*5-methyl group in thymine. Methyl groups in the major groove (as in *C*5-methylcytosine, thymine, or *N*6-methyladenine) decrease the BII substate population of RpY steps. Due to methylation a clearer distinction of the BI substate stability between YpR and RpY (CpG/GpC or TpA/ApT) steps arises. A positive correlation between the BII substate population and base stacking distances is seen only for poly(GC). A methyl group added into the major groove increases mean water residence times around the purine N7 atom, which may stabilize the BI substate by improving the hydration network between the DNA backbone and the major groove. The *N*6-methyl group also forms a water molecule bridge between the N6 and O4 atoms, and thus further stabilizes the BI substate.

1. Introduction

Biological processes at the molecular level are dominated by protein−DNA recognition. Useful information on the binding specificity of various protein−DNA complexes is provided by crystallographic, spectroscopic, and modeling studies.[1−7] However, the DNA contributions to the recognition process are not fully understood. Proteins have to recognize specifically their cognate DNA sequence. The recognition process consists of sequence characteristic DNA backbone behavior, in addition to direct readout mechanisms. In B-DNA there are two conformational backbone substates, BI and BII, which are commonly defined by ϵ and ζ angles. The BI substate corresponds to $\epsilon - \zeta$ with the minimum energy around −90°. $\epsilon - \zeta$ around +90° is the minimum for the BII state.[8,9] This definition is generally limited to free B-DNA[10] with canonical α and γ (g−/g+) angles. It has been proposed that these two backbone angles (α and γ) are unlikely to flip spontaneously in free B-DNA,[10] but can adopt an unusual conformation in A-DNA and complexed B-DNA.

The idea that the sequence dependence of the dynamic DNA backbone behavior plays a decisive role in the early recognition process[11,12] is consistent with earlier observations[13] and recent results.[14] As the backbone conformation is important for an early state of the recognition process, one might expect that the DNA sequence specificity can be expressed by its conformational backbone substates. The atomic content of the sugar phosphate backbone is uniform for all nucleotides; hence, the sequence specificity of the DNA backbone requires specific base−base interactions. The BI/BII interconversions show correlations with altered phosphate group positions, groove parameters, stacking properties, and helical parameters.[15−17] Stacking properties of dinucleotides for each different base step will be different and sensitive to the base modification. It has been shown that each dinucleotide step has a different stacking energy. This is reflected in the population of the BII substate.[15] Base stacking in connection with sequence specificity is mainly considered as the important factor for the preferred backbone conformation. Different hypotheses have been proposed concerning the sequence dependency of B-DNA backbone conformations based on the base stacking interactions including the effects of neighboring sequences[15] or exocyclic groups.[18]

Additional exocyclic groups as in *C*5-methylcytosine, *N*4-methylcytosine, and *N*6-methyladenine nucleobases (Figure 1) have been found in DNA from various natural sources. The methylation of DNA plays a role in a variety of biological processes, including regulation of gene expressions, DNA replication, mismatch repair, and defense against foreign DNA.[19] So far in metazoa methylation is found only on C5 of cytosine, occurring in CG sequences,[19] while N6-methylation of adenine in GATC or GANTC (with N for any base) sequences is involved in the pathogenicity of different bacteria.[20−22] Information concerning the structural and dynamical influences of C5-methylation of cytosine and N6-methylation of adenine might be an advantage for antibacterial drug design.

These two types of DNA methylation, at C5 of cytosine and N6 of adenine, are inducing different structural effects in their natural occurrences. C5-methylation of cytosine does not influence the DNA curvature,[7] while N6-methylation of adenine may enhance DNA curvature that is modulated by properly phased GATCs in certain sequences.[23] In addition, C5 and N6 methyltransferases require different bending angles of their cognate DNA sequences for a proper interaction.[24] Methylation of the CpG step freezes the amplitude of phosphate mo-

* To whom correspondence should be addressed. E-mail: Klaus.Liedl@uibk.ac.at.

[†] Permanent address: Chemistry Department, Faculty of Mathematics and Natural Sciences, Sebelas Maret University, Surakarta, Indonesia.

10.1021/jp048519v CCC: $30.25
Published on Web 12/14/2004

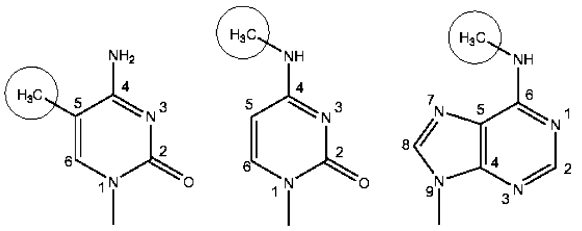

Figure 1. Chemical structures of methylated DNA bases: (left) *C*5-methylcytosine, (middle) *N*4-methylcytosine, and (right) *N*6-methyladenine.

tions,[7,25,26] which in turn reduces the flexibility of the B-DNA backbone. Besides these differences, a cleavage of the TCGA sequence was presumed to be protected by the influence of a methyl group on N6 of TCG6mA on the DNA backbone.[27] The distance between this methyl group to the backbone (±9 Å) is too far for a strong direct interaction. Thus, we surmise that the change of base stacking and hydration properties due to methylation is involved in the effect on the DNA backbone.

Water migration from the ionic phosphate to the sugar oxygen is related to the BI/BII transition.[28] The migration mediates signal transduction from the minor to the major groove.[29] It has been shown that a changed hydration pattern in the minor groove leads to a different BI/BII substate pattern.[18] It has been proposed that the BI substate in *C*5-methylcytosine is stabilized by a water-bridged contact between one free phosphorus oxygen and the *C*5-methyl group.[30] This hypothesis suggests an influence of water molecules on the BI/BII transition. In an attempt to assess more details about the impact of methylation on the DNA backbone, we have compared the effects of the *C*5-methyl group of pyrimidine and the *N*6-methyl group of adenine on the backbone behavior and the hydration network by simulating four different B-DNA dodecamers ($d(GC)_6$, $d(AT)_6$, $d(G(5mCG)_5C)$, and $d(A(T6mA)_5T)$).

2. Methods

Structural and dynamical properties of biologically interesting macromolecules such as DNA have been extensively studied by means of molecular dynamics (MD) simulation.[31−34] This method provides an excellent tool for investigation of biomolecules in their biologically active form. The inclusion of the long-range interactions via the Ewald summation in the form of the particle mesh Ewald method and improved parametrization of the force fields (implemented in the AMBER program) allow stable calculation of B-form DNA trajectories[35−37] in the nanosecond time range. The rate of interconversion between BI/BII substates of DNA is on the subnanosecond time scale,[28,38,39] and allows an exhaustive description of this conformational aspect by computer simulations.

3. Computational Details

Four different dodecamers, $d(GC)_6$, $d(AT)_6$, $d(G(5mCG)_5C)$, and $d(A(T6mA)_5T)$), and one additional control sequence, $d(AU)_6$, were created with NUCGEN on the basis of standard B-DNA parameters. The parametrizations of the *N*6-methyladenine and uracil were carried out in analogy to the existing parameters for adenine and thymine, respectively, in the AMBER force field (parm99). Charges were derived using the RESP[40,41] charge-fitting procedure (multiconformational RESP). The ab initio electrostatic potential for RESP was calculated using GAUSSIAN98[42] at the HF/6-31G* level of theory (parametrization details are available in the Supporting Information). Equivalent sodium ions for charge neutralization were added using the XLEAP module in AMBER7.[43] Subsequently, solvation of the DNA structure with TIP3P Monte Carlo water boxes requiring a 12 Å solvent shell in all directions resulted in a rectangular unit cell containing about 4000−5000 TIP3P water models. The simulations were carried out using the AMBER7 package with the all-atom force field of Cornell et al.[44] and the modifications of Cheatham et al.[45] and Wang et al.[41] Standard protocols from previous extensive simulations[46−48] were adapted for our needs.

First, 500 steps of minimization were carried out with harmonic restraints of 25 kcal mol^{-1} $Å^{-2}$ on the DNA and counterion positions. During the following five 100-step minimizations the restraints on the counterions were relaxed faster than on the DNA. Finally 500 steps of unrestrained minimization were carried out. For the equilibration a similar procedure was applied. After the constant-volume system was heated for 20 ps from 50 to 300 K and the DNA and ion positions were kept constant with harmonic restraints of 25 kcal mol^{-1} $Å^{-2}$ on the DNA and counterion positions, the harmonic restraints were reduced throughout the following 25 ps, faster on the counterions than on the DNA using constant-pressure and constant-temperature conditions. Finally 5 ps of unrestrained equilibration was carried out before the trajectory was generated for further simulation times. The temperature bath coupling was achieved by the Berendsen algorithm.[49]

General simulation parameters were kept constant during the whole simulation: temperature of 300 K, pressure of 1 atm, 2 fs time step, SHAKE constraints of 0.00005 Å on all bonds involving hydrogen atoms, 9 Å nonbonded cutoff, and 0.00001 convergence criterion for the Ewald part of the nonbonded interactions. The structural information was collected every 500 steps (1 ps). All simulations were performed on an SGI Origin 3800.

The resulting trajectory was analyzed with the AMBER7 package, and snapshots were investigated with different visualization programs, i.e., RASMOL,[50] CHIMERA,[51] and VMD.[52] The MD Toolchest was used for the calculation of the helical parameters[53] and for visualization in the form of graphs.[54] To gain thermodynamic and kinetic information from the coordinates of an MD trajectory, we count how often $\epsilon - \zeta$ of every nucleotide is in a certain angle space (16°), resulting in a 22 bin histogram. The values are interpolated, and the resulting smoothed curve shows two maxima defining two phosphate conformations, BI and BII. By combining all values of the same base steps, we assume that our trajectories will be long enough to sufficiently sample the phase space and thus yield the partition function (Z). Transforming the curves into free energy graphs [$\Delta G = -RT \ln(Z)$] resulted in ΔG and $\Delta G^{\ddagger}$ values for every base step. The water molecule arrangement in the grooves is described by the radial distribution of the water oxygen atoms, the mean water residence time, and the water density map. The water residence time is defined by the lifetime of hydrogen bonds to any hydrogen bond donor/acceptor atom in the grooves with a 3.5 Å distance and a 120° angle cutoff. The water density maps are drawn by taking the N7 atom as the center of a grid box. The water densities are calculated from the water occupancy for each grid. For this purpose, the trajectories are filtered for two adjacent phosphates (P and P + 1) populating just the BI substate.

4. Results

After standard minimization and equilibration procedures, the two dodecamers ($d(GC)_6$ and $d(G(5\ mCG)_5C)$) were simulated for 14950 ps. The other two dodecamers, ($d(AT)_6$ and

TABLE 1: DNA Helical Parameters Calculated from the Different MD Trajectories[a]

param	$d(GC)_6$	$d(G(5mCG)_5C)$	$d(AT)_6$	$d(A(T6mA)_5T)$
x_{disp} (Å)	-0.64 ± 0.04	-1.02 ± 0.02	-1.05 ± 0.46	-0.37 ± 0.34
inclination (deg)	-3.50 ± 1.76	-0.15 ± 0.47	-7.88 ± 3.90	-9.51 ± 2.31
tip (deg)	-1.14 ± 4.72	0.11 ± 2.27	-0.56 ± 5.76	0.73 ± 2.18
shear (Å)	0.01 ± 0.06	-0.01 ± 0.06	0.91 ± 1.21	-0.04 ± 0.21
stretch (Å)	0.14 ± 0.02	0.20 ± 0.02	-0.26 ± 1.12	0.13 ± 0.04
stagger (Å)	0.13 ± 0.10	-0.03 ± 0.06	-0.36 ± 0.33	-0.07 ± 0.09
buckle (deg)	0.34 ± 2.91	-0.2 ± 3.09	0.74 ± 4.93	-0.41 ± 7.06
propeller twist (deg)	-10.97 ± 4.00	-10.32 ± 1.36	-11.17 ± 5.87	-9.76 ± 2.30
opening (deg)	0.14 ± 0.71	1.51 ± 0.48	5.36 ± 1.42	6.37 ± 1.46
shift (Å)	0.02 ± 0.14	0.00 ± 0.14	0.04 ± 0.32	-0.10 ± 0.18
slide (Å)	-0.18 ± 0.20	-0.12 ± 0.29	0.03 ± 0.41	-0.15 ± 0.42
rise (Å)	3.44 ± 0.20	3.35 ± 0.12	3.50 ± 0.21	3.52 ± 0.20
tilt (deg)	0.04 ± 1.78	-0.07 ± 1.45	0.12 ± 2.87	0.27 ± 2.10
roll (deg)	5.97 ± 7.54	4.65 ± 3.25	8.85 ± 5.93	6.28 ± 4.84
twist (deg)	32.42 ± 1.77	33.24 ± 4.38	32.77 ± 7.73	31.65 ± 5.86

[a] Values are given as averages ± standard deviations.

$d(A(T6mA)_5T)$), were simulated for 24950 ps due to their less populated BII conformer. From the total energy observation, each system equilibrates after at least 500 ps of simulation time. Thus, the last 14000 and 24000 ps of each trajectory are taken for analysis. In both polynucleotides, poly(GC) and poly(AT), methylation only slightly changes the root-mean-square deviation (RMSD) of all heavy atoms with respect to the canonical B-DNA. Methylation in poly(AT) decreases the average RMSD value from 3.99 to 2.97 Å, while methylation in poly(GC) does not cause any significant change in the average RMSD value (~2.80 Å). On the other hand, the RMSD values of the methylated sequences with respect to the nonmethylated ones of their equilibrated state are nearly zero. This difference might indicate different consequences of the additional methyl groups for the two sequences.

Neither experimental nor theoretical studies on the C5-methylation of cytosine reveal extensive changes in the DNA curvature,[7] while *N*6-methyladenine is able to enhance the DNA curvature exhibited by the GATC sequence.[23] Our results show only slight modification of the DNA curvature, both in poly(GC) and in poly(AT). Most of the helical parameters do not show significant alterations due to methylation (Table 1). The most distinctive modification of a helical parameter due to base methylation is the base displacement along the *x*-axis (x_{disp}). The x_{disp} values increase due to methylation in poly(AT), but decrease in poly(GC). Global x_{disp} values are sensitive to the percentage of BII population. If the BII substate population is about 20%, the global x_{disp} is positive, which means the bases are displaced toward the major groove.[55] Therefore, the change of the global x_{disp} should reflect the change of the total BII substate percentage. In an attempt to understand the influence of methyl groups on the DNA backbone behavior, the evaluation of the simulation results is divided into three parts.

4.1. Stabilization−Destabilization of the BI Substate. An analysis of ϵ and ζ angles as the main determinants of BI and BII substates has been performed. An α and γ angle analysis has also been performed. Most of the dinucleotide steps exhibit constant canonical α and γ (g−/g+) angles. In free B-DNA noncanonical α and γ angles are rarely encountered, but appear more frequently in protein−DNA complexes.[10,55−57] In the present simulation study, the end-standing base pairs and one base step next to the end-standing base pairs exhibit noncanonical α and γ angles. These noncanonical α and γ angles, except those found at the end-standing base pairs, are only observed in our simulation of nonmethylated DNA. In the poly(GC), α and γ angles do not influence the $\epsilon - \zeta$ value.[30] The noncanonical α and γ angles which are observed in poly(AT) result in unusual $\epsilon - \zeta$ angles. These angles lie within BI and BII substates. Therefore, an exclusion of all base steps which exhibit noncanonical α and γ angles is preferred for poly(AT) strands to remove a possible influence on the BI/BII transition process.

We calculated the percentage of BII ($\epsilon - \zeta \geq 90°$) population for each base step and compared the different values. Unlike the GpC and CpG steps, the BII propensities of the ApT and TpA steps (Figure 2) are not significantly different. The additional methyl group on the N6 atom of adenine clearly distinguishes the ApT steps from the TpA steps concerning their BII propensity. Similar to the methyl group on the C5 atom of cytosine, the N6 methyl group decreases the number of BII substates on RpY steps and increases it for YpR steps. Considering the number of methyl groups in the major groove, poly(AT) and poly(G5mC), both have one methyl group on the C5 position of the pyrimidine base. This similarity might cause the similar BII percentages on ApT and Gp5mC base steps. On the other hand, TpA and 5mCpG base steps exhibit a large difference concerning the BII populations. A shorter distance between the C5 methyl group and the phosphate group of the RpY steps compared to the distance in the YpR steps might result in a stronger influence on the backbone conformation of the RpY steps.

After the evaluation of the BI/BII substate probability, we investigated the influence of a methyl group on the free energy of BI/BII transitions in poly(AT). The histogram analysis results in a smooth ΔG curve. To estimate the convergence of the free energy values, we carried out the analysis for two consecutive time blocks (Figure 3). These results indicate that our data sufficiently sample the phase space of BI/BII transitions. The transition state is defined from the maximum point of the ΔG curves, and the forward transition barriers are plotted. Figure 3 displays a similar but smaller free energy alteration of the ApT and TpA steps due to methylation compared to that of GpC and CpG steps. The BI substate of RpY steps is thermodynamically and kinetically stabilized in both types of methylation.

The TpA step has been claimed to behave differently concerning its BI/BII transitions compared to other YpR steps.[15] In our work we do not find any differences of the TpA step compared to the CpG step, neither in the thermodynamic nor in the kinetic parameters. The ΔG values of ApT and TpA steps are indistinguishable, while the values of GpC and CpG steps show clear differences. Due to N6-methylation of adenine, a clearer distinction of these two steps is possible. Interestingly, the free energy for BI/BII transition of RpY steps seems to correlate with the number of methyl groups occurring in the

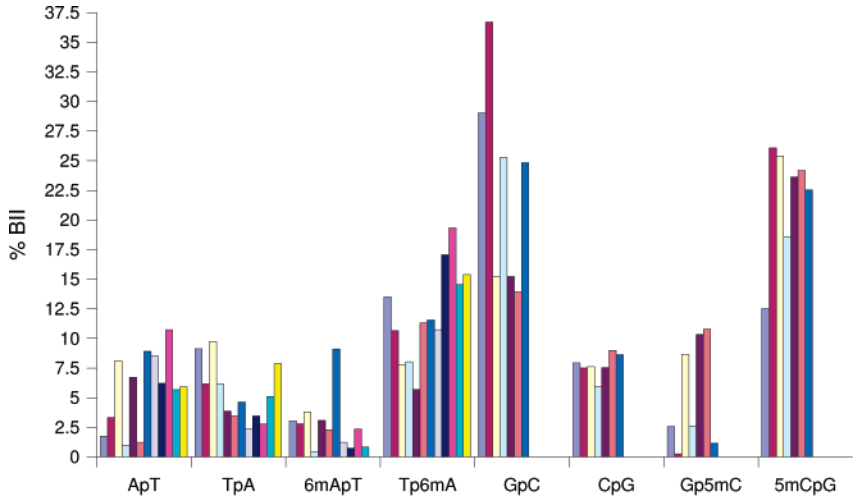

Figure 2. Percentage of BII population for each base step in 2 ns time intervals drawn as a histogram.

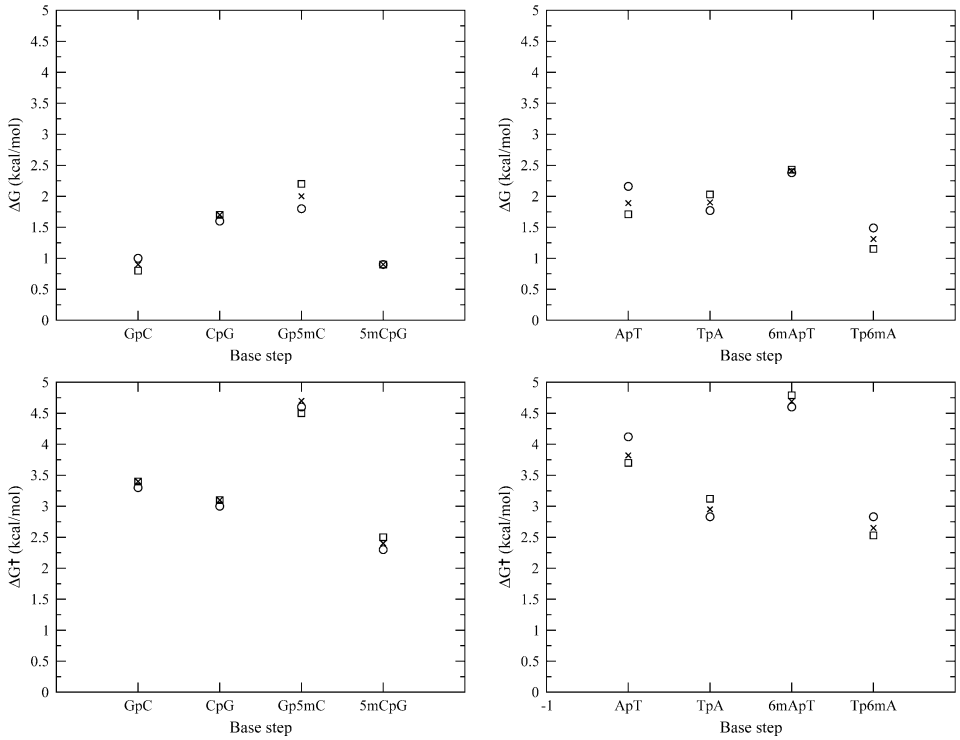

Figure 3. (Top) Δ*G* values (kcal/mol) for the BI/BII transition of the base steps ApT/6mApT and TpA/Tp6mA. Times signs correspond to the values of the whole trajectories, squares correspond to data from the first half trajectories, and circles correspond to data from the second half trajectories. (Bottom) The same notation as in the top panel for the BI/BII forward transition barrier (Δ$G^{\ddagger}$) values (kcal/mol) is used. Data for the C5-methylation of cytosine are taken from Rauch et al.[30]

major groove. GpC steps have the lowest Δ*G* value (0.91 ± 0.29 kcal/mol), followed by Gp5mC (1.82 ± 0.19 kcal/mol) and ApT (1.84 ± 0.13 kcal/mol) steps. 6mApT steps exhibit two methyl groups in the groove and show the highest Δ*G* value (2.48 ± 0.42 kcal/mol). Thus, methyl groups in the major groove seem to exert an additive effect on the BI stability of the RpY steps.

Unlike the nearly indistinguishable GpC and CpG steps (time evolution of $\epsilon - \zeta$ available in the Supporting Information), the BI/BII transition barrier energies of ApT and TpA steps are clearly sequence dependent. YpR base steps undergo BI/BII transitions more easily compared to RpY steps. Due to methylation the Δ$\Delta G^{\ddagger}$ values increase for both sequences. The addition of a *C*5-methyl group on cytosine increases the Δ$\Delta G^{\ddagger}$ value for the GpC/CpG steps (∼2 kcal/mol), whereas the *N*6-methyl group only slightly changes the Δ$\Delta G^{\ddagger}$ value for the ApT/TpA steps (∼1 kcal/mol). This feature indicates that the *C*5-methyl group plays an important role in the kinetic stabilization of BI/BII transitions. But how this methyl group presents its influences on the phosphate backbone behavior remains unclear.

4.2. Base Stacking Distance and BI/BII Transition Correlation. The BII conformation decreases the base stacking, which means an increase of x_{disp}, twist, or base stacking distance. The base stacking distance is similar to the rise parameter, but it involves only one DNA strand. The distance is defined as a normalized distance between C1′ atoms from two adjacent nucleotides. Due to the limited occurrence of facing BII substates, the rise will be less altered compared to the base stacking distance. The base stacking distance is plotted as a function of BII population to examine its correlation (Figure 4). C5-methylation of cytosine increases the average base stacking distance on the CpG step and decreases it on the GpC

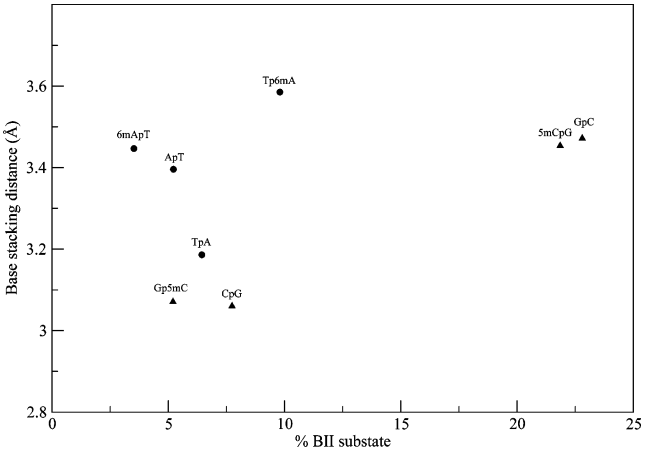

Figure 4. Base stacking distances as a function of BII percentage for each base step. The distance is defined as a normalized distance between C1′ atoms from two adjacent nucleotides.

TABLE 2: Summary of the Hydration Parameters of the Hydrogen Bond Donor/Acceptor Atoms in Poly(AT) and Poly(GC)[a]

	coordination number	first hydration shell (Å)	mean water residence time[b] (ps)
	Poly(AT) and Poly(6mAT)		
O1P(ApT)	3.28 (3.38)	2.70 (2.70)	4.2 (4.2)
O2P(ApT)	3.30 (3.30)	2.70 (2.70)	4.8 (4.6)
O1P(TpA)	3.17 (3.27)	2.70 (2.70)	4.2 (4.3)
O2P(TpA)	3.32 (3.31)	2.70 (2.70)	4.9 (5.0)
major groove			
N7	1.04 (0.96)	2.85 (2.90)	5.4 (7.5), 5.8[c]
O4	1.23 (1.05)	2.75 (2.75)	4.6 (12.3), 1.7[c]
N6	4.70 (6.14)	3.00 (4.80)	1.1 (1.0)
H61			1.3 (1.0)
H62			3.0 (−)
minor groove			
N3	1.07 (1.07)	2.85 (2.85)	4.5 (4.4)
O2	1.43 (1.46)	2.75 (2.75)	4.3 (4.4)
	Poly(GC) and Poly(G5mC)		
O1P(GpC)	3.11 (3.31)	2.70 (2.70)	4.3 (4.0)
O2P(GpC)	3.50 (3.45)	2.70 (2.70)	4.4 (4.5)
O1P(CpG)	3.18 (3.20)	2.70 (2.70)	4.1 (4.3)
O2P(CpG)	3.39 (3.34)	2.70 (2.70)	4.8 (4.7)
major groove			
N7	1.32 (1.11)	2.85 (2.85)	3.3 (4.7)
O6	1.47 (1.25)	2.75 (2.75)	3.0 (3.6)
N4	3.98 (3.59)	3.00 (3.10)	1.1 (1.1)
H41			1.01 (1.0)
H42			3.4 (2.5)
minor groove			
N3	1.07 (1.00)	2.85 (2.90)	3.9 (3.9)
O2	1.10 (1.05)	2.75 (2.75)	6.2 (5.2)
N2	4.90 (4.84)	3.00 (3.00)	1.1 (1.1)
H21			1.0 (1.0)
H22			2.7 (2.8)

[a] Values in parentheses represent the hydration parameters for poly(6mAT) and poly(G5mC), respectively. The end-standing bases are excluded. [b] Mean values from 10 nucleobases for the mentioned donor/acceptor hydrogen bond atoms. [c] Mean water residence times from 5000 ps simulation of $d(AU)_6$.

step. This correlation cannot be seen in poly(AT). The small average base stacking distance alteration is in line with the relatively unchanged average rise of poly(GC). The excluded base step in poly(AT) due to the noncanonical α and γ angles might contribute to the difference between the averages of the rise and base stacking distance. The base stacking distances of 6mApT and ApT steps are about the same as those of 5mCpG and GpC steps, while the BII propensities are as low as those of Gp5mC and CpG. The BI/BII transition in poly(GC) is more

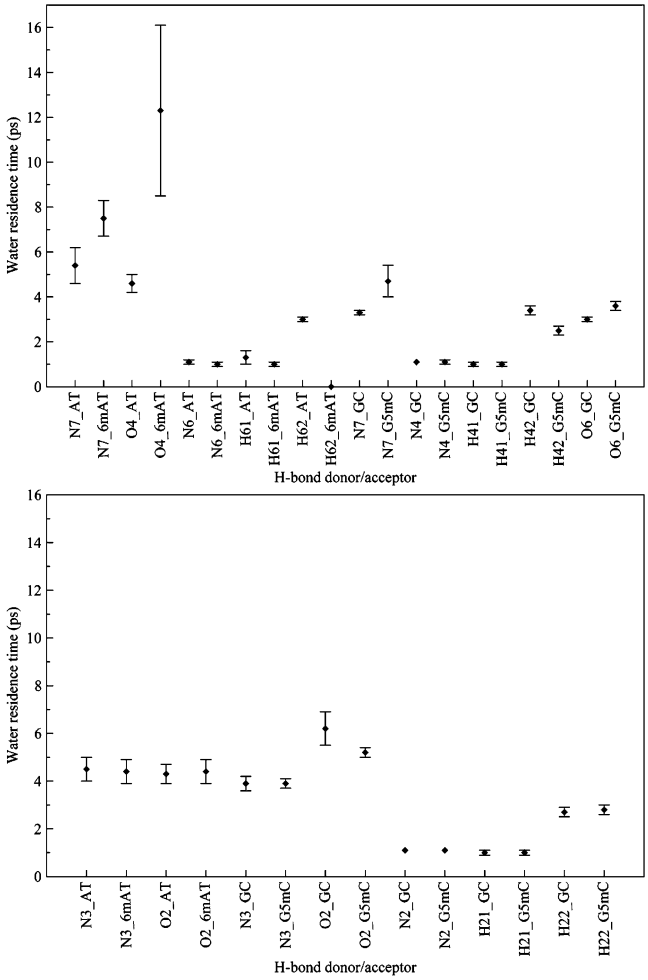

Figure 5. (Top) Major groove hydration. (Bottom) Minor groove hydration. The lifetime of hydrogen bonds between water molecules and hydrogen bond donor/acceptor atoms in the grooves in two different methylation states are plotted as mean values from 10-nucleobase average residence times for the mentioned donor/acceptor hydrogen bond atoms. The bars in the graphs represent standard deviation values of the mean water residence time for each base.

sensitive to the change of base stacking distance compared to the transition in poly(AT). Due to methylation the BII population of the TpA step increases only slightly, while for the CpG step the BII population is increased from about 8% to 23% and the base stacking distance increases by about 0.4 Å.

An additional methyl group on the C5 atom of cytosine changes the base stacking distance in correlation with the change of the BII substate population. This methyl group gives larger base stacking distances for the 5mCpG step compared to the Gp5mC step. In contrast to this feature, the *C*5-methyl group on thymine gives a lower base stacking distance for TpA steps compared to ApT steps. An additional methyl group on the N6 atom of adenine only increases the base stacking distance for the TpA step without a significant correlation with the BII population. Besides the base stacking distance, slide and twist angles also have an influence on defining backbone conformations.[15] But both types of methylation change slide and twist angle preferences only slightly. Thus, we conclude that there might be another driving factor for the altered BII propensity which can be perturbed by a methyl group.

4.3. Effects of Methylation on DNA Hydration. The correlation between BI/BII transition and hydration in the grooves[18,28,29] has led to further analysis of the hydration changes induced by methylation. Introducing a methyl group in the major

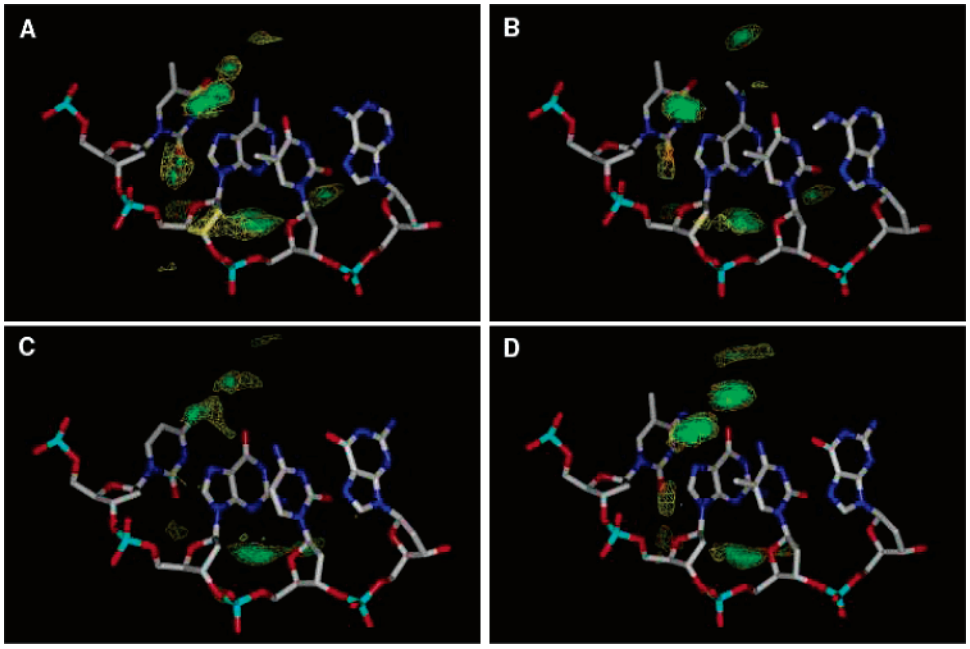

Figure 6. Water density maps of methylated and nonmethylated poly(AT) and poly(GC), illustrating the hydration network in the major groove. The N7 atom is the center of a 30 × 30 × 30 Å^3 grid box. The higher water density (30% maximum density) is presented in solid green, while the lower (20% maximum density) is in yellow mesh. Key: (A) poly(AT), (B) poly(6mAT), (C) poly(GC), (D) poly(G5mC).

groove surely will change the hydration pattern. As a hydrophobic moiety, the methyl group will shift water molecules away from their positions. Despite this property, the difference in electronegativity between hydrogen and carbon atoms provides a weak proton donor for a hydrogen bond. Thus, the hydration pattern of the DNA molecule can also be changed due to the ability of methyl groups to hydrogen bond with water molecules.

A comparison of the hydration parameters of methylated and nonmethylated DNA sequences is summarized in Table 2. The hydration of the phosphorus oxygen and all hydrogen bond donor/acceptor atoms in the grooves has been analyzed. None of these hydration sites show any significant change concerning the radius of the first hydration shell. A slight water coordination number change on the phosphorus oxygen atom, pointing to the minor groove (O1P), is not seen for the other phosphorus oxygen atom (O2P). The mean water residence times around the O2P atom are slightly longer than the mean water residence times around the O1P atom. The coordination number behaves similarly and is higher for O2P. From this point of view the stabilization of the BI substate involving hydration is not clear.

A methyl group on C5 of pyrimidine was expected to be able to stabilize a water molecule bridge to the phosphorus oxygen which points into the major groove (O2P).[30] If the stabilization of the BI conformer is due to a bridging water molecule, then the residence time of water molecules which bind to the O2P atom should increase. But the mean water residence time around the O2P atoms is constant. On the other hand, methylation obviously induces significant changes in the major groove hydration. Clearer changes of water residence times in the grooves can be seen in Figure 5. The *C*5-methyl groups stabilize water molecules around the N7 and O6 atoms of guanine. The mean water residence time of the cytosine amino group is decreased around the hydrogen atom, which points to the *C*5-methyl group. In poly(AT), N6-methylation of adenine increases the stability of water around the N7 atom and O4 atoms. As methyl groups are weak proton donors, they seem to stabilize water molecules around hydrogen bond acceptor atoms which are closer than 4 Å to the C atom of the methyl group. But in the same distance, the C-5 methyl group destabilizes water molecules around hydrogen bond donor atoms.

Both types of methylation increase the mean water residence time around the N7 atom in the major groove of purine bases. The value of the methylated poly(GC) is close to the value of the poly(AT), and it increases due to N6-methylation. An increase of the water residence time around the N7 atom is in line with the increasing BI stability of RpY steps due to methylation. The *C*5-methyl group of thymine does not show an influence on the water residence time around the N7 atom. This *C*5-methyl group stabilizes water molecules around the O4 atom of thymine. Due to N6-methylation this hydration site becomes even more stable. Thus, due to the methylation of adenine the hydration of the O4 atom is altered stronger compared to the hydration site around N7. As the O4 atom lies in the center of the major groove this finding indicates a smaller influence of N6-methylation on the backbone flexibility, but rather an importance for direct sequence recognition. With the addition of the *N*6-methyl group an inhomogeneous environment is introduced to the center of the major groove, which is reflected in the large standard deviation of the mean water residence time around the O4 atom in poly(6mAT). However, most of the helical parameters are not changed significantly due to their type of methylation.

Methylation does not change the hydration of the poly(AT) minor groove, while in poly(GC) methylation reduces the mean water residence time on O2 of cytosine. Though, the mean residence time on O2 of *C*5-methylcytosine (5.2 ps) is still higher than in thymine (4.3 ps), C5-methylation of cytosine decreases the average mean water residence time for the whole minor groove to 4.6 ps, which is similar to the minor groove value for poly(AT) (4.4 ps). The difference in poly(GC) is probably due to the effect of the amino group in the minor groove as was previously observed.[18,58] Methyl groups in C5 increase base stacking distances, which results in an increasing distance between the minor groove amino groups and the O2 atom. This change will destabilize a possible water hydrogen

bound to the O2 atom in poly(GC) and is possibly related to the destabilization of BI substates in 5mCpG steps.

Similar effects on hydration due to both types of methylation in the alternate purine−pyrimidine sequences can be seen for the N7 hydration site. The distance of the N7 atom to the following 3′-phosphate group is about 7 Å. For such a long distance, a single water bridge cannot be the reason for the stabilization of the BI substate. Figure 6 shows the major groove hydration network around the RpY step, which indicates a possible mechanism of the BI substate stabilization due to methylation. One purine base in the center of the strand is taken as a static reference for the calculation of the water density map. The trajectories are filtered to exclude BII substates on the phosphate backbone before and after the static reference, resulting in a minimum trajectory length of 8000 ps. The water density map is drawn in a $30 \times 30 \times 30$ Å^3 grid box with the N7 atom as the center of the box. When a methyl group is attached to the C5 position of pyrimidine (panels A, B, and D of Figure 6), a water network connects the N7 atom and the phosphorus oxygen of the RpY steps. This hydration network does not exist in panel C of Figure 6, where no methyl group occurs in the major groove.

Panels A and B in Figure 6 present different densities of the hydration network. A lower density is shown in panel B, which means the *N*6-methyl seems to destabilize the hydration network. The *N*6-methyl group has stabilized the hydration around the N7 atom of adenine, but the water density near the phosphorus oxygen of the TpA steps is reduced and the BI substate is destabilized. Besides hydration sites which are directly connected to the backbone, the water molecules bridge the two exocyclic groups in the major grooves (N6 and O4 atoms) in the methylated sequence. This water molecule bridge could be the reason for the increase of the base stacking, which in turn means either a decrease of the base stacking distance or less twisted or less shifted ApT steps.

5. Summary and Conclusions

Molecular dynamics simulations of four different dodecanucleotides ($d(GC)_6$, $d(AT)_6$, $d(G(5mCG)_5C)$, and $d(A(T6mA)_5T)$) have been carried out for a total of 80 ns simulation time. Methylation changes the RMSD of poly(AT) slightly with respect to the canonical B-DNA and does not influence this RMSD of poly(GC). Neither of the two types of methylation alter the helical parameters significantly, except the global x_{disp}. Thus, the RMSD difference due to the N6-methylation may come from the sum of each helical parameter's slight alteration. These findings are in line with the previous observations that the C5-methylation of CpG does not significantly change the DNA curvature,[7,30] and the *N*6-methyladenine may enhance the bend of the GATC sequence.[23]

Among the slight alterations of the helical parameters, the global x_{disp} shows the most distinctive alteration due to methylation. Due to N6-methylation the global x_{disp} is increased, but the C5-methylation decreases it. As this parameter is correlated with the BII substate population, the effects of methylation on the DNA backbone behavior are investigated. Interestingly, both methylations show a similar effect on the BII population for each step, but the effects are weaker in poly(AT) compared to poly(GC). The free energy evaluation of BI/BII transitions indicates a thermodynamic and kinetic stabilization of the BI substate for the RpY steps due to methylation. The free energy for BI/BII transitions of RpY steps seems to correlate with the number of methyl groups occurring in the major groove (GpC $<$ Gp5mC $\approx$ ApT $<$ 6mApT). Thus, methyl groups in the major groove seem to exert an additive effect on the BI stability of the RpY steps.

We found that both types of methylation affect BI/BII transitions. Additions of exocyclic bulky groups such as methyl groups will perturb the intrastrand base stacking interactions. As has been proposed, the BI/BII transitions are dependent on the dinucleotide sequence, which is mainly governed by the intrastrand base stacking interactions.[15] Our results show a good correlation between the base stacking distances and the BI/BII transitions in poly(GC), but this is not the case for poly(AT). Therefore, the change of the base stacking distance does not sufficiently explain the effect of methylation on the BI/BII transitions.

The correlation between BI/BII transition and hydration in the grooves has led to further analysis on the hydration changes induced by methylation. The stabilization of the BI substate at the CpG step due to methylation was previously explained by an ideal distance for one water molecule bridging the phosphorus oxygen and the methyl group. This hypothesis is not supported by a longer mean water residence time on this site. The mean water residence times in the major groove seem to be related to the number of methyl groups occurring in the major groove. Both types of methylation increase the mean water residence time around the N7 atom in the major groove of purine bases. When a methyl group is attached to the C5 position of pyrimidine, a water network connects the N7 atom and the phosphorus oxygen of the RpY steps; hence, the BI substate is stabilized. The *N*6-methyl group of adenine further increases the mean water residence time around N7 purine ring atoms and forms a water molecule bridge between N6 and O4 atoms. The formation of this water molecule bridge might increase the base stacking, and the BI substate is more stabilized. As the O4 atom lies in the center of the major groove this finding indicates a smaller influence of N6-methylation on the backbone flexibility, but rather an importance for direct sequence recognition.

Acknowledgment. This work was supported by a grant from the Austrian Science Fund (Project Number P16176) and a scholarship from the Austrian Federal Ministry for Education, Science and Culture for F.R.W.

Supporting Information Available: Parametrization details and time evolution of $\epsilon - \zeta$. This material is available free of charge via the Internet at http://pubs.acs.org.

References and Notes

(1) Chen, S.; Vojtechovsky, J.; Parkinson, G. N.; Ebright, R. H.; Berman, H. M. *J. Mol. Biol.* **2001**, *314* (1), 63−74.
(2) Luscombe, N.; Austin, S.; Berman, H.; Thornton, J. *Genome Biol.* **2000**, *1* (1), REVIEWS001.
(3) Smith, S. A.; McLaughlin, L. W. *Bioorg. Chem.* **1999**, *27*, 215−26.
(4) Jenkins, T.; Lane, A. *Biochim. Biophys. Acta* **1997**, *1350* (2), 189−204.
(5) Sunnerhagen, M.; Denisov, V.; Venu, K.; Bonvin, A.; Carey, J.; Halle, B.; Otting, G. *J. Mol. Biol.* **1998**, *282* (4), 847−58.
(6) Byun, K.; Beveridge, D. *Biopolymers* **2004**, *73* (3), 369−79.
(7) Derreumaux, S.; Chaoui, M.; Tevanian, G.; Fermandjian, S. *Nucleic Acids Res.* **2001**, *29* (11), 2314−26.
(8) Hartmann, B.; Lavery, R. *Q. Rev. Biophys.* **1996**, *29* (4), 309−68.
(9) Fratini, A.; Kopka, M.; Drew, H.; Dickerson, R. *J. Biol. Chem.* **1982**, *257* (24), 14686−707.
(10) Varnai, P.; Djuranovic, D.; Lavery, R.; Hartmann, B. *Nucleic Acids Res.* **2002**, *30* (24), 5398−406.
(11) Wellenzohn, B.; Flader, W.; Winger, R.; Hallbrucker, A.; Mayer, E.; Liedl, K. R. *Biochemistry* **2002**, *41* (12), 4088−95.
(12) Wellenzohn, B.; Flader, W.; Winger, R.; Hallbrucker, A.; Mayer, E.; Liedl, K. R. *J. Am. Chem. Soc.* **2001**, *123* (21), 5044−9.

(13) Smith, S.; McLaughlin, L. *Biochemistry* **1997**, *36*, 6 (20), 6046−58.
(14) Lamoureux, J.; Maynes, J.; Glover, J. *J. Mol. Biol.* **2004**, *335* (2), 399−408.
(15) Bertrand, H.; Ha-Duong, T.; Fermandjian, S.; Hartmann, B. *Nucleic Acids Res.* **1998**, *26* (5), 1261−7.
(16) Srinivasan, A.; Olson, W. *J. Biomol. Struct. Dyn.* **1987**, *4* (6), 895−938.
(17) Hartmann, B.; Piazzola, D.; Lavery, R. *Nucleic Acids Res.* **1993**, *21* (3), 561−8.
(18) Wellenzohn, B.; Flader, W.; Winger, R.; Hallbrucker, A.; Mayer, E.; Liedl, K. R. *Nucleic Acids Res.* **2001**, *29* (24), 5036−43.
(19) Jeltsch, A. *ChemBioChem* **2002**, *3* (4), 274−93.
(20) Reisenauer, A.; Kahng, L.; McCollum, S.; Shapiro, L. *J. Bacteriol.* **1999**, *181* (17), 5135−9.
(21) Robertson, G.; Reisenauer, A.; Wright, R.; Jensen, R.; Jensen, A.; Shapiro, L.; Roop, R., II. *J. Bacteriol.* **2000**, *182* (12), 3482−9.
(22) Reisenauer, A.; Shapiro, L. *EMBO J.* **2002**, *21* (18), 4969−77.
(23) Polaczek, P.; Kwan, K.; Campbell, J. *Mol. Gen. Genet.* **1998**, *258* (5), 488−93.
(24) Garcia, R.; Bustamante, C.; Reich, N. *Proc. Natl. Acad. Sci. U.S.A.* **1996**, *93* (15), 7618.22.
(25) Geahigan, K.; Meints, G.; Hatcher, M.; Orban, J.; Drobny, G. *Biochemistry* **2000**, *39* (16), 4939−46.
(26) Meints, G.; Drobny, G. *Biochemistry* **2001**, *40* (41), 12436−43.
(27) Zebala, J.; Choi, J.; Trainor, G.; Barany, F. *J. Biol. Chem.* **1992**, *267* (12), 8106−16.
(28) Winger, R. H.; Liedl, K. R.; Rudisser, S.; Pichler, A.; Hallbrucker, A.; Mayer, E. *J. Phys. Chem. B* **1998**, *102* (44), 8934−40.
(29) Flader, W.; Wellenzohn, B.; Winger, R.; Hallbrucker, A.; Mayer, E.; Liedl, K. R. *J. Phys. Chem.* **2001**, *105* (42), 10379−87.
(30) Rauch, C.; Trieb, M.; Wellenzohn, B.; Loferer, M.; Voegele, A.; Wibowo, F.; Liedl, K. R. *J. Am. Chem. Soc.* **2003**, *125* (49), 14990−1.
(31) von Kitzing, E. *Methods Enzymol.* **1992**, *211*, 449−67.
(32) Beveridge, D. L.; Ravishanker, G. *Curr. Opin. Struct. Biol.* **1994**, *4*, 246−55.
(33) Feig, M.; Pettitt, B. *J. Mol. Biol.* **1999**, *286* (4), 1075−95.
(34) Castrignano, T.; Chillemi, G.; Desideri, A. *Biophys J.* **2000**, *79*, 1263−72.
(35) Young, M. A.; Nirmala, R.; Srinivasan, J.; McConnell, K. J.; Ravishanker, G.; Beveridge, D. L.; Berman, H. M. *Structural Biology: The State of the Art*, Proceedings of the 8th Conversation; Adenine Press: Albany, NY, 1994.
(36) Cieplak, P.; Cheatham, T. E., III; Kollman P. A. *J. Am. Chem. Soc.* **1997**, *119*, 6722−30.
(37) Cheatham, 3rd, T.; Kollman, P. *J. Mol. Biol.* **1996**, *259* (3), 434−44.
(38) Trieb, M.; Rauch, C.; Wellenzohn, B.; Wibowo, F.; Loerting, T.; Liedl, K. R. *J. Phys. Chem. B* **2004**, *108* (7), 2470−6.
(39) Trieb, M.; Rauch, C.; Wellenzohn, B.; Wibowo, F.; Loerting, T.; Liedl, K. R. *J. Phys. Chem. B* **2004**, *108* (32), 12258.
(40) Bayly, C. I.; Cieplak, P.; CornellW, D.; Kollman, P. A. *J. Phys. Chem.* **1993**, *97*, 10269−80.
(41) Wang, J.; Cieplak, P.; Kollman, P. A. *J. Comput. Chem.* **2000**, *21* (12), 1049−74.
(42) Gaussian98 (Revision A.1): Frisch, M. J.; Trucks, G. W.; Schlegel, H. B.; Scuseria, G. E.; Robb, M. A.; Cheeseman, J. R.; Zakrzewski, v. G.; Montgomery, J. A.; Stratmann, R. E.; Burant, J. C.; Dapprich, S.; Milliam, J. M.; Daniels, A. D.; Kudin, K. N.; Strain, M. C.; Farkas, O.; Tomasi, J.; Petersson, G. A.; Ayala, P. Y.; Cui, Q.; Morokuma, K.; Malick, D. K.; Rabuck, A. D.; Raghvachari, K.; Foresman, J. B.; Cioslowski, J.; Ortiz, J. V.; Stefanov, B. B.; Liu, G.; Liashenko, A.; Piskorz, P.; Komaromi, I.; Gomperts, R.; Martin, R. L.; Fox, D. J.; Keith, T.; Al-Laham, M. A.; Peng, C. Y.; Nanayakkara, A.; Gonzalez, C.; Challacombe, M.; Gill, P. M. W.; Johnson, B. G.; Chen W.; Wong, M. W.; Andres, J. L.; Head-Gordon, M.; Replogle, E. S.; Pople, J. A., Gaussian, Inc., Pittsburgh, PA, 1995.
(43) AMBER 7: Case, D. A.; Pearlman, D. A.; Caldwell, J. W.; Cheatham, T. E. III.; Wang. J.; Ross, W. S.; Simmerling, C. L.; Darden, T. A.; Merz, K. M.; Stanton, R. V.; Cheng, A. L.; Vincent, J. J.; Crowley, M.; Tsui, V.; Gohlke, H.; Radmer, R. J.; Duan, Y.; Pitera, J.; Massova, I.; Seibel, G. L.; Singh, U. C.; Weiner, P. K.; Kollman, P. A., University of California, San Francisco, 2002.
(44) Cornell, W. D.; Cieplak, P.; Bayly, C. I.; Gould, I. R.; Merz, K. M.; Ferguson, D. M.; Spellmeyer, D. C.; Fox, T.; Caldwell, J. W.; Kollman, P. A. *J. Am. Chem. Soc.* **1995**, *117*, 5179−97.
(45) Cheatham, 3rd, T.; Cieplak, P.; Kollman, P. *J. Biomol. Struct. Dyn.* **1999**, *16* (4), 845−62.
(46) Young, M. A.; Ravishanker, G.; Beveridge, D. L. *Biophys. J.* **1997**, *73*, 2313−36.
(47) Flader, W.; Wellenzohn, B.; Winger, R.; Hallbrucker, A.; Mayer, E.; Liedl, K. R. *Biopolymers* **2003**, *68* (2), 139−49.
(48) Cheatham, 3rd, T.; Young, M. *Biopolymers* **2000**, *56* (4), 232−56.
(49) Berendsen, H. J. C.; Postma, J. P. M.; van Gunsteren, W. F.; DiNola, A.; Haak, J. R. *J. Chem. Phys.* **1984**, 81.
(50) Rasmol 2.7.2.1: Sayle, R., Glaxo Wellcome Medicines Research Centre, Hertfordshire, U.K., 2001.
(51) Petterson, E. F.; Goddard, T. D.; Huang, C. C.; Couch, G. S.; Greenblatt, D. M.; Meng, E. C.; Ferrin, T. E. *J. Comput. Chem.* **2004**, *25*, 1605−1612.
(52) Humphrey, W.; Dalke, A.; Schulten, K. *J. Mol. Graphics* **1996**, *14* (1), 33−8, 27−8.
(53) Lavery, R.; Sklenar, H. *J. Biomol. Struct. Dyn.* **1988**, *6* (1), 63−91.
(54) Ravishanker, G.; Swaminathan, S.; Beveridge, D.; Lavery, R.; Sklenar, H. *J. Biomol. Struct. Dyn.* **1989**, *6* (4), 669−99.
(55) Djuranovic, D.; Hartmann, B. *J. Biomol. Struct. Dyn.* **2003**, *20* (6), 771−88.
(56) Djuranovic, D.; Hartmann, B. *Biopolymers* **2004**, *73* (3), 356−68.
(57) Packer, M.; Hunter, C. *J. Mol. Biol.* **1998**, *280* (3), 407−20.
(58) Lankas, F.; Cheatham, T., III; Spackova, N.; Hobza, P.; Langowski, J.; Sponer, J. *Biophys. J.* **2002**, *82* (5), 2592−609.